BMC Plant Biology

RESEARCH

Open Access

Extracellular DNA triggers glucosinolate-dependent defence responses against *Frankliniella occidentalis*

Leila Rassizadeh[1], Antoni Garcia-Molina[2], Victor Flors[1], Isaac Vega-Muñoz[1*] and Jordi Gamir[1*]

Abstract

Background Extracellular self-DNA (exDNA) perception activates innate immunity in plants, inducing resistance to various agricultural pathogens and pests with different lifestyles. However, the mechanisms behind exDNA-induced immunity are yet to be understood. Our previous results showed a noticeable reduction in *Frankliniella occidentalis* (western flower thrips) feeding symptoms in *Arabidopsis thaliana* treated with exDNA. In this study, we aim to gain a deeper understanding of the mechanisms mediating exDNA-induced resistance against *F. occidentalis*.

Results Treatment with extracellular exDNA led to notable transcriptional changes in plants. In the absence of herbivore challenge, exDNA-treated plants showed enrichment of genes involved in fatty acid biosynthesis, whereas after thrips infestation, these plants exhibited stronger activation of several defence-related metabolic pathways, particularly those associated with both aliphatic and indolic glucosinolate (GSL) biosynthesis. Furthermore, measurement of thrips feeding damage in exDNA-treated and control plants revealed that exDNA-induced resistance (exDNA-IR) was abolished in aliphatic GSL-deficient mutants.

Conclusion The early accumulation of GSLs, including glucobrassicin and glucoraphanin, in exDNA-treated plants, together with their further increase after infestation, indicates that these plants are primed for a faster and stronger defence response upon herbivore attack. Genetic analyses revealed that exDNA-induced resistance is abolished in aliphatic glucosinolate-deficient mutants, while indolic glucosinolate deficient plants partially retain resistance, demonstrating that aliphatic glucosinolates are involved in exDNA induced immunity against thrips. This study advances our understanding of the mechanisms underlying the plant's response to exDNA as a danger signal and demonstrated its contribution to induced resistance against thrips herbivory.

Keywords Extracellular DNA, Induced resistance, Damage-associated molecular patterns (DAMPs), *Frankliniella occidentalis*, Transcriptomic analysis, Glucosinolates, *Arabidopsis thaliana*

*Correspondence:
Isaac Vega-Muñoz
ivega@uji.es
Jordi Gamir
jgamir@uji.es
[1]Plant Immunity and Biochemistry group, Department of Biology Biochemistry and Natural Sciences, Universitat Jaume I, Avd. Vicente Sos Baynat s/n, Castelló 12071, Spain
[2]Centre for Research in Agricultural Genomics (CRAG) CSIC-IRTA-UAB-UB, C/Vall Moronta, Edifici CRAG, Barcelona, Bellaterra (Cerdanyola del Vallès) 08193, Spain

Introduction

Plant immunity relies on two immune responses: pattern-triggered immunity (PTI) and effector-triggered immunity (ETI) [1]. PTI provides the first layer of defence against non-adapted pathogens by detecting pathogen-associated molecular patterns (PAMPs) through pattern recognition receptors (PRRs). On the other hand, ETI, the second immune strategy, is triggered by the recognition of pathogen effector molecules by plant resistance (R) gene products [1, 2]. However, PTI is not solely activated by PAMP recognition; it can also be triggered by various molecules from different sources, functioning as danger signals, such as damage-associated molecular patterns (DAMPs) [3, 4]. DAMPs are host-derived molecules that are released to the extracellular space due to cell disruption caused by factors such as physical injuries, pathogen attacks, and herbivores. Some examples of well-studied DAMPs in plants are cytosolic proteins, peptides, nucleotides, and some oligomeric fragments of plant cell wall polysaccharides [5, 6]. The detection of these relocated molecules through intact neighbouring cell receptors initiates general signalling pathways, enabling plants to respond effectively to a wide array of challenges [5, 6]. In the last years, several studies have suggested that extracellular self-DNA (exDNA) acts as a DAMP, triggering unspecific defence responses in plants and potentially hindering plant root growth [7–10]. Despite the impact of exDNA on plant defence, the specific receptors for exDNA recognition remain elusive, leaving key questions about perception and underlying mechanisms unanswered [11].

Recent studies have reported the capacity of exDNA to induce resistance against various bacterial and fungal pathogens [12–19]. However, the impact of exDNA on agricultural pests has not been thoroughly assessed. Our previous work demonstrated exDNA-induced resistance (exDNA-IR) against thrips herbivory in *Arabidopsis thaliana* [20].The western flower thrips *Frankliniella occidentalis* (Thysanoptera: Thripidae) is a widespread agricultural pest causing "silvering damage" on plants and serves as a vector for economically important viruses, such as the tomato spotted wilt virus (TSWV) [21, 22]. Plant defences against herbivory encompass both direct mechanisms, such as specialized structures, phytohormones, secondary metabolites, and proteins with toxic or repellent properties, as well as indirect defences. Indirect defences involve the release of plant volatiles, also known as Volatile Organic Compounds (VOCs), to attract the natural enemies of herbivores [23–26]. Among phytohormones, jasmonic acid (JA) plays a pivotal role in inducing plant resistance against leaf-chewing and piercing–sucking insects [22, 23, 27] and, in concert with other signalling molecules, regulates the synthesis of secondary metabolites that can ultimately impede herbivory [28]. Glucosinolates (GSLs) are one of the well-studied defence metabolites in brassicaceous plants. Upon herbivore damage, the degradative enzyme myrosinase, initially stored in separate cells and compartments, is released and generates GSLs breakdown products that induce resistance against a wide range of attackers [29–31].

It has been demonstrated that exDNA induces early plant defence responses. This includes the depolarization of the plasma membrane, generation of reactive oxygen species (ROS) bursts, and phosphorylation of MAP kinases [7, 32, 33]. Moreover, in *Lactuca sativa* plants, both self exDNA and non-self exDNA treatments from *Capsicum chinense* resulted in significant changes in CpG DNA hypomethylation and inducing the upregulation of defence-related genes [34]. Similarly, upregulation of JA biosynthesis genes in *Arabidopsis thaliana* and *Solanum lycopersicum* following self-exDNA treatment has been reported [16]. In Arabidopsis, self-exDNA treatment induced the expression levels of JA-related genes, while the nonself-exDNA treated group exhibited more differentially expressed genes (DEGs) but not a detectable JA response [35]. The amplitude of the exDNA-IR depending on the source of DNA has not been resolved yet: some studies reported comparable plant response to both self-DNA (from host plants) and nonself-DNA (from other organisms) treatments [34, 36] while others observed a stronger response to self-DNA treatment [7, 37]. The perception and mechanisms distinguishing self-DNA from nonself-DNA remain largely elusive in plants; however, some hypothetical exDNA recognition pathways have been recently proposed, providing a foundation for future studies [11].

Here, we provide evidence highlighting the impact of exDNA treatment on transcriptomic changes and the induction of GSLs in the exDNA-IR phenomenon against thrips herbivory. Recently, the ability of exDNA to induce resistance against pathogens and pests has been reported [20]. However, the specific molecular pathways involved in this resistance have remained unexplored. Conducting a comprehensive transcriptomic analysis following exDNA treatment and thrips infestation is crucial to gaining a deeper understanding of the mechanisms behind exDNA-induced immunity. Our findings aim to provide insights into the mechanisms of exDNA-induced immunity.

Materials and methods

Biological materials

Arabidopsis thaliana Col-0 seeds and GSL deficient mutants in the same genetic background, *myb28/29*, *cyp83a1* (aliphatic GSL deficient) and *cyp79b2/b3* (indolic GSL deficient), previously described [38–41] were obtained from the Nottingham Arabidopsis Stock Centre (NASC). Plants were grown in growth chambers

under short-day conditions (8 /16 light/dark photoperiod at 22 °C, 70% relative humidity).

A laboratory colony of western flower thrips (*Frankliniella occidentalis*) was reared on fresh bean pods under room temperature conditions.

DNA extraction and plant treatment

Genomic DNA was extracted from *A. thaliana* Col-0 leaves following the procedure described by Duran-Flores and Heil [33], with some modifications. In summary, plant material was ground in liquid nitrogen, and 4 ml of extraction buffer (200 mM Tris–HCl pH 7.5, 250 mM NaCl, 25 mM EDTA-Na_2, 0.5% SDS) was added per 1 g of plant fresh weight. The samples were kept at room temperature for 45 min, followed by a 10-minute centrifugation at 14,000 rpm. Subsequently, an equal volume of isopropanol was added to the samples and kept at -20 °C for 1 h. After a 10-minute centrifugation at 13,000 rpm, the pellet was washed twice with 70% ethanol (5 min, 13,000 rpm), dried, and then dissolved in 50 µL of nuclease-free water. The quality and concentration of the extracted DNA were checked at 260 nm using a NanoDrop (Thermo Scientific, Wilmington, DE, USA). Before treatment, the DNA underwent sonication using an ultrasonic bath (NAHITA 610/6 ultrasonic) for 15 min at a maximum amplitude (40–50 kHz). A concentration of 150 µg mL^{-1} was applied by spraying onto the surface of the 5-6-week-old Arabidopsis plants.

Experimental design and thrips infestation

Five to six week old Arabidopsis plants were used for all experiments. To evaluate the effects of exDNA and thrips infestation on Arabidopsis, plants were treated with either exDNA or water (control). Twenty four hours after treatment, plants were either infested by placing 15 first instar thrips larvae by plant or left uninfested.

For transcriptomic analyses, plant material was harvested 7 h post-infestation (hpi), for glucosinolate quantification, samples were collected 7 and 24 hpi. At each sampling point, whole rosettes were harvested and immediately frozen in liquid nitrogen. For each biological replicate, whole rosettes from three individual plants were collected and pooled to form one sample. A total of five biological replicates were processed for each treatment.

For phenotypic assays, rosette leaves were harvested 4 days post infestation (dpi) and scanned to quantify the thrips feeding damage (silver-gray patches). Images analysis was performed using llastik and Fiji [42–44]. For each genotype, 10 individual plants were infested with 15 thrips larvae per plant, and the assays were repeated at least three times. Each experiment was independently repeated at least three times, and data from all biological replicates were pooled for statistical analyses.

RNA extraction and RNA-seq analysis

RNA was extracted from 100 mg frozen plant material using RNeasy plant mini kit (Qiagen) following the protocol provided by the manufacturer, and the supernatant was diluted in 50 µL RNase-free water. The RNA concentration was determined by absorbance at 260 nm using a NanoDrop spectrophotometer (Thermo Scientific, Wilmington, DE, USA). The RNA integrity number (RIN) value was verified for the quality of RNA extraction before sequencing analysis. The transcriptome sequencing has been assessed by Macrogen, Inc. (Seoul, South Korea). Messenger RNA was enriched from total RNA by poly(A) selection, and strand-specific RNA-seq libraries were prepared using the TruSeq Stranded mRNA LT Sample Prep Kit according to the manufacturer's protocol. Libraries were sequenced in paired-end mode (151 bp) on an Illumina HiSeq 2500 platform. Trimmed reads were mapped to the reference genome (TAIR10) with HISAT2. After the read mapping, StringTie was used for transcript assembly. Differentially expressed genes (DEGs) were identified using DESeq2, with transcripts showing an absolute fold change ≥ 2 and an adjusted P value ≤ 0.05 (Wald test) considered significant. Transcriptome expression profiles were analyzed to identify transcripts whose expression responses depended on the combined effect of exDNA treatment and thrips infestation. These transcripts were identified using a two-way ANOVA testing the interaction between exDNA treatment and infestation ($P \leq 0.05$), as described by Garcia-Molina et al. [45]. Heatmaps with hierarchical clustering were drawn using normalised read counts Fragments Per Kilobase Milion (FPKM) according to the Ward D2 algorithm with the R package *pheatmap* (version 1.0.12). Heatmap partition to retrieve general gene clustering was optimised by *k*-means. Gene Ontology (GO) and *Kyoto Encyclopedia of Genes and Genomes* (KEGG) pathway enrichment analyses were performed using DAVID (Database for Annotation, Visualization, and Integrated Discovery) (https://davidbioinformatics.nih.gov/) and ShinyGO 0.77 (https://bioinformatics.sdstate.edu/go77/). RNAseq data has been submitted into NCBI Sequence Read Archive (SRA) with accession number: PRJNA1373521.

Glucosinolates quantification

Frozen plant material was ground in liquid nitrogen. For extraction, 1 mL of methanol was added per 100 mg of tissue in a 10 mL tube. As an internal standard, 100 µL of previously desulfonated sinigrin was added to each sample. The tubes were incubated in a water bath at 90 °C for 5 min, cooled on ice for 15 min, and then filtered through a 0.2 µm syringe filter. Lastly, samples were diluted 10-fold with milli-Q grade water before analysis.

Preparation of desulfonated sinigrin: For 10 samples, 670 µL of 1.2 mM sinigrin solution was loaded onto a DEAE-Sephadex A-25 column. The column was washed twice with 1 mL of 67% methanol, followed by two washes with 1 mL of 20 mM sodium acetate buffer (NaOAc, pH 5.5). Subsequently, 100 µL of sulfatase solution was loaded into the column, followed by 100 µL of sodium acetate buffer. The column was incubated overnight at room temperature. Desulfonated sinigrin was then eluted twice with 0.5 mL of 60% methanol.

The separation of GSL was final optimized performed using a HPLC Kinetex C18 analytical column with a 5 µm particle size, 2.1 100 mm (Phenomenex). The column oven was maintained at a constant temperature of 40 °C. The injection volume was 5 µL, and the auto-sampler was operated under a thermostatic condition of 10 °C.

The mobile phase consisted of a mixture of (A) water and (B) acetonitrile both supplemented with formic acid (0.1%, v/v). The gradient elution program was as follows: (i) 0.01–1.00 min (95%A, v/v); (ii) 1.00–3.00 min (95%A-5%A, v/v); (iii) 3.00–4.00 min (5%A); (iv) 4.00–5.00 min (5%A, v/v-95%A, v/v); (v) 5.00–6.00 min (95%A, v/v).

MS/MS conditions

The quantification of glucosinolates was performed in an Acquity ultra-performance liquid chromatography system (UPLC) (Waters, Mildford, MA, USA), connected to a triple quadrupole mass spectrometer (TQS, Waters, Manchester, UK). The mass spectrometer was equipped with an ESI source in negative ion mode, utilizing the following optimized parameter settings: a source desolvation temperature of 650 °C, a source cone voltage of 25 V, a source capillary voltage of 2.2 kV, and a source desolvation gas flow rate of 1200 L/Hr. All acquired data were collected in the Multiple Reaction Monitoring (MRM) mode. The Masslynx 4.2 software was employed to optimize the mass spectrometry method by directly infusing 100 µg/L standard solutions into the mass spectrometer. The MS ions and corresponding MS/MS transitions monitored for each compound are extracted from Crocoll et al. [46].

Statistical analyses

The normality of the data was assessed using Shapiro-Wilk's test. For datasets exhibiting a normal distribution, a one-way analysis of variance (ANOVA) was carried out, followed by Fisher's least significant difference (LSD) test. For nonparametric data, the Kruskal-Wallis test was performed, followed by pairwise Mann-Whitney tests for multiple comparisons. All statistical analyses were conducted using the R programming language (version 4.2.2). The *ggplot2* R package (version 3.4.0) was used for the data visualization. The P-value of < 0.05 was considered statistically significant.

Results

The application of exDNA treatment leads to important transcriptome reconfigurations to ameliorate the response against thrips infestation

In our recent research, we observed the effect of exDNA treatment on enhancing plant resistance against thrips, leading to a remarkable decrease in symptoms associated with feeding areas [20]. To gain some insight into the global gene expression changes triggered by exDNA treatment and herbivory, an RNA-Seq profiling was conducted on leaves collected from four distinct experimental groups, namely control and exDNA-treated plants with and without thrips infestation. The infestation was performed 24 h after exDNA treatment, and the thrips were allowed to feed on the plants for 7 h before harvesting the samples. Multidimensional scaling (MDS) analysis mainly discriminated samples under infestation from the controls (component 1, 48.2% total variance), indicating that the main source of variability among samples was the infestation by thrips (Fig. 1a). However, the application of exDNA also led to prevalent differences in both control and infested plants (component 2, 26.1% total variance). Furthermore, as demonstrated in the hierarchical clustering analysis, expression patterns in exDNA-treated plants closely resemble each other, as do those of the control plants, regardless of the presence or absence of herbivory (Fig. 1b).

Based on these results, we analysed gene expression profiles in more detail. The normalized expression values of transcripts showing a significant interaction between exDNA treatment and thrips infestation ($P \leq 0.05$, two-way ANOVA; 6,490 genes) were used to generate a heatmap with hierarchical clustering (Fig. 1c). Transcripts in cluster 2 displayed antagonistic patterns between exDNA treated plants and control plants (regardless of infestation), whereas those in the cluster 4 showed a similar steady-state upon infestation, although exDNA treatments imposed different basal levels (Fig. 1c). The most remarkable differences in the expression patterns between exDNA treated plants, with and without thrips infestation, were in clusters 1, 3, and 5 (Fig. 1c). Functional annotation in metabolic pathways of the coresets of transcripts within those clusters was carried out according to significant enrichment in KEGG terms (adjusted $P \leq 0.1$, Fisher's Exact test).

Cluster 1 transcript levels are steady between groups except for the exDNA-infested plants where there is a clear down regulation (Fig. 1c), these genes were related to key biological processes such as glyoxylate and dicarboxylate metabolism (supplementary Fig. S1). Within this pathway, we found the Glycolate Oxidase (*GOX*) family of genes such as *GOX1* and *GOX2* and some photosynthesis-related genes, like the Ribulose bisphosphate carboxylase (small chain) family protein (*RBCS*) including

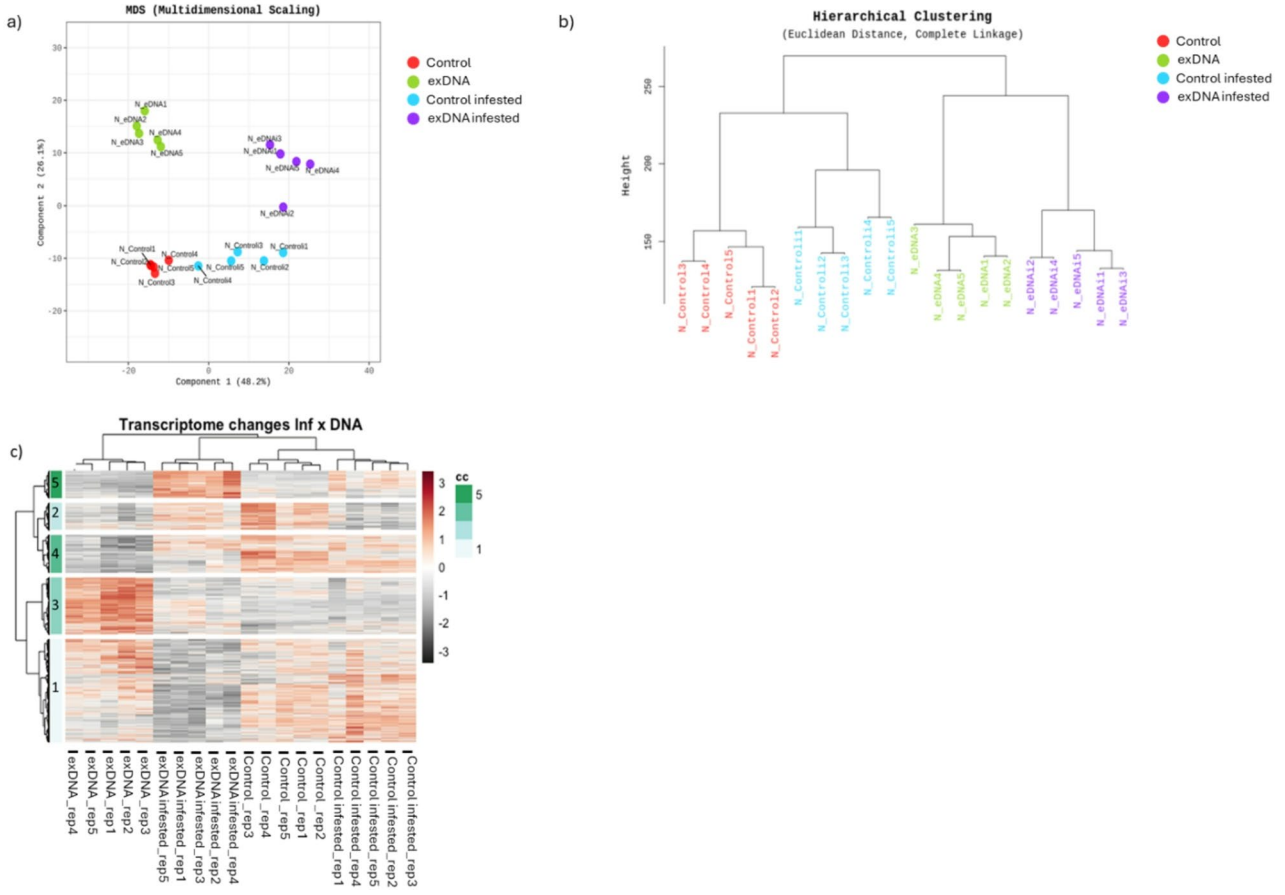

Fig. 1 Differential gene expression patterns following exDNA treatment and thrips infestation. **a** MDS plot shows variation among RNA-Seq samples; distance between sample labels indicates dissimilarity of expression pattern between groups. **b** Hierarchical clustering analysis shows the similarity in the expression pattern between groups. Using each sample normalized value, the high expression similarities were grouped together (Distance metric = Euclidean distance, Linkage method= Complete Linkage). **c** Heatmap of normalized FPKM values of genes significantly enriched in each sample (p-value ≤ 0.05, two-way ANOVA), hierarchical clustering using Ward D2 method with K-mean. Each row represents a gene ID, and each column represents a sample including exDNA, eDNA-treated-infested, Control and Control infested. The colour and intensity of the boxes in the heatmap indicate changes in gene expression relative to a reference value. High-expression genes are shown in red on the map; low-expression genes are shown in grey

RBCS1B and *RBCS2B*; gene list provided in (Supplementary Table S1). The transcripts in cluster 3 displayed higher levels in plants treated with exDNA but lowered upon infestation as in non-exDNA treated plants (Fig. 1c). Those transcripts retrieved significant enrichment in different KEGG pathways such as pathways associated with fatty acid elongation, metabolism, and biosynthesis (supplementary Fig. S1). Within them, we observed enrichment of the β-Ketoacyl-CoA synthetase (*KCS*) gene family (*KCS10*, *KCS12*, *KCS16*, *KCS19*, *KCS4*, *KCS5*, *KCS6* and, *KCS8*), a rate-limiting enzyme in the synthesis of very long-chain fatty acids (VLCFAs) in plants [47]. We also observed enrichment of the long-chain acyl-CoA synthetase (*LACS*) family, including *LACS1* and *LACS2*, which are involved in the synthesis of wax and cutin and are therefore essential for plant stress resistance [48] (Supplementary Table S1).

Finally, cluster 5 encompassed transcripts with an enhanced accumulation in response to the infestation, being the exDNA-infested plants the ones with a clear enhanced transcript accumulation to all the groups, while the exDNA treatment alone did not show changes in comparison to its control.

Among the KEGG pathways identified for this core set of transcripts, the most highly enriched term was the glucosinolate (GSL) biosynthesis pathway (Fig. 2a), comprising 14 genes highlighted in Fig. 2b. These genes belong to different branches of the glucosinolate biosynthetic pathway and are mapped onto the KEGG glucosinolate pathway overview shown in Fig. 2c. In addition, the alpha-linolenic acid synthesis pathway was significantly enriched, including well-known components of the jasmonate pathway such as lipoxygenases (*LOX2*, *LOX3*, *LOX4*, *LOX6*), allene oxide synthase (*AOS*), allene oxide cyclases (*AOC1–AOC4*), oxophytodienoate reductase 3 (*OPR3*) (Supplementary Table S1). It's worth noting that alpha-linolenic acid is an unsaturated fatty acid closely linked to plant antioxidant mechanisms and the

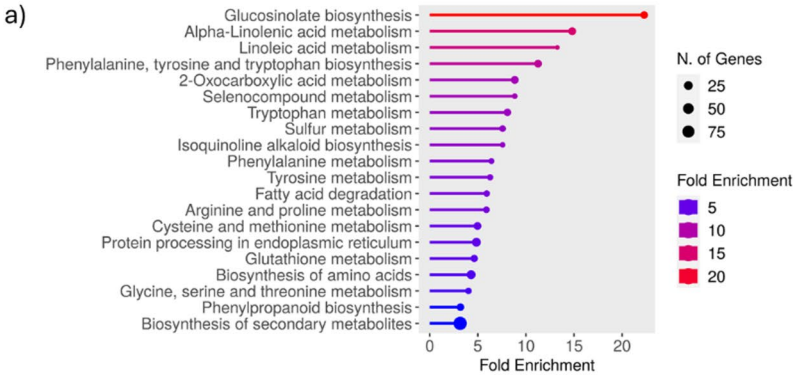

b)

	eDNA					eDNA-infested					Control					Control-infested				
BCAT4	105.8	120.4	105.5	144.5	142.5	268.6	228.7	264.6	259.0	234.1	131.1	134.8	114.9	131.2	125.0	226.6	171.9	186.2	152.5	209.9
MAM1	322.4	253.4	285.0	255.8	306.7	388.8	320.0	339.6	343.4	320.1	195.0	188.1	185.9	207.7	202.2	161.2	172.8	152.0	230.5	227.3
IIL1	160.7	143.6	156.4	142.5	168.9	196.1	167.4	179.0	159.3	173.4	128.7	126.2	140.2	133.8	127.6	106.9	111.4	103.3	138.0	140.3
CYP79B3	14.4	12.8	12.1	14.9	15.0	70.9	64.4	71.1	99.2	75.8	16.8	17.5	19.8	18.4	18.9	60.1	47.6	38.6	29.0	42.9
CYP79B2	11.8	10.4	9.6	13.0	11.0	48.2	42.0	44.8	66.7	47.2	14.5	14.1	17.1	16.8	15.3	37.9	37.9	31.4	22.4	34.8
CYP79F1	177.0	142.1	163.6	133.1	186.5	202.1	169.8	191.0	175.8	175.6	126.4	123.0	120.1	124.3	118.8	89.2	95.1	81.5	131.0	130.3
CYP79F2	1.6	1.5	1.3	1.8	2.2	4.7	3.5	4.2	3.4	3.5	2.3	2.1	2.3	2.5	2.1	2.8	2.3	3.0	3.1	3.4
CYP83B1	92.1	79.6	66.5	77.9	80.9	211.4	194.1	170.4	244.8	220.3	94.1	90.8	105.8	110.5	95.5	180.1	159.9	129.1	94.2	133.7
CYP83A1	241.0	198.0	220.0	187.9	241.1	259.5	242.2	244.1	234.5	228.5	171.9	167.5	170.5	187.3	177.3	140.3	145.6	126.9	174.2	179.5
SUR1	78.5	69.0	70.1	60.2	74.9	99.2	81.8	90.1	88.6	90.5	58.1	54.7	59.1	62.0	55.0	56.8	56.4	53.2	63.0	62.2
UGT74B1	47.9	46.0	43.7	43.0	45.1	61.4	51.7	55.0	60.9	57.7	32.2	31.6	33.7	33.8	33.5	33.5	31.6	26.8	35.1	34.7
SOT16	28.6	25.0	22.8	25.9	24.9	66.5	61.0	56.7	83.8	67.3	25.8	23.7	29.4	28.9	26.4	52.2	50.5	40.9	35.1	45.8
SOT17	18.0	19.1	18.2	25.6	26.4	44.6	38.8	40.5	42.8	37.8	27.2	26.6	25.7	25.3	25.3	36.1	34.6	35.3	32.9	41.6
SOT18	70.4	67.6	68.7	68.1	77.1	83.9	77.3	76.0	77.0	73.5	50.4	52.2	54.5	52.0	52.1	43.0	42.1	39.9	54.9	53.6

FPKM 400 300 200 100 0

c)

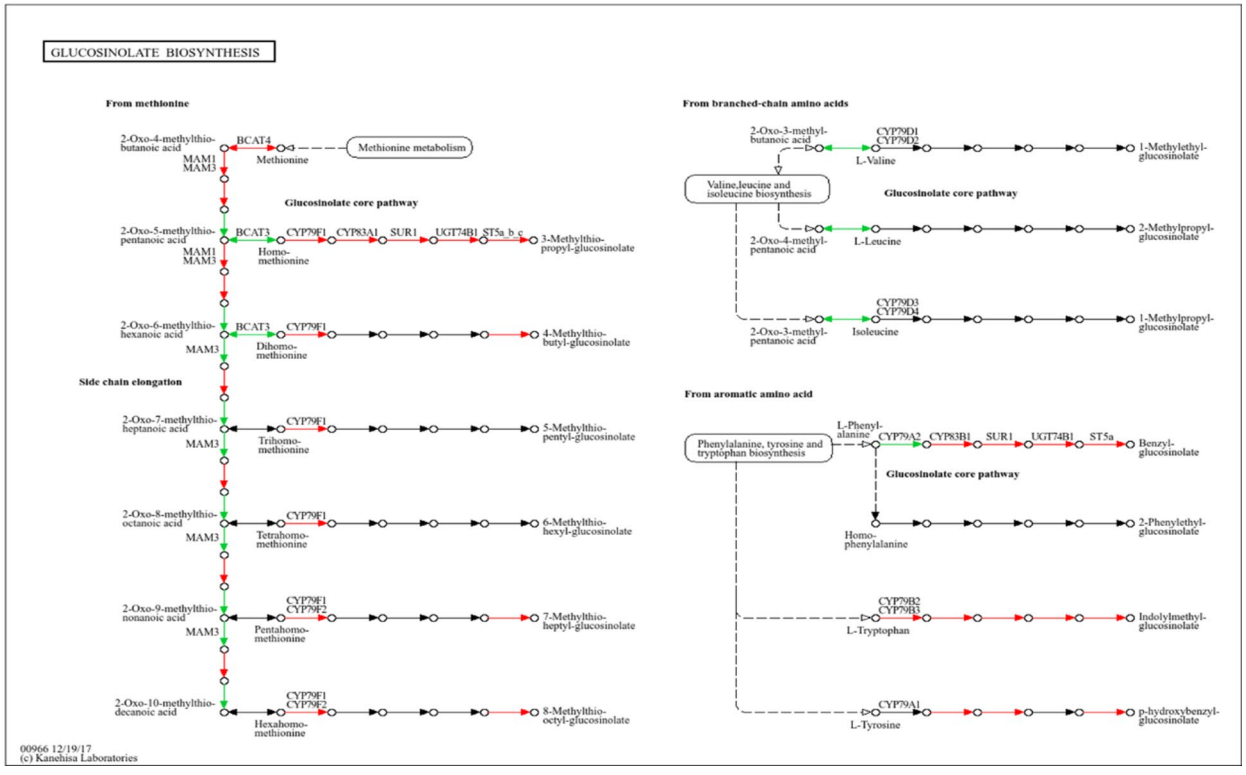

Fig. 2 (See legend on next page.)

(See figure on previous page.)

Fig. 2 Glucosinolate enrichment in *A.thaliana* following exDNA treatment and herbivory. **a** The top enriched GO terms for Cluster 5 sorted by fold enrichment levels and number of genes pathway enrichment. Point size indicates the number of genes associated with each GO term, and color represents fold enrichment values ranging from low (blue) to high (red). analysis were carried out using ShinyGO software v 0.77. **b** The heatmap represents the enrichment pattern for each gene in the glucosinolate pathway in different treatments presented in log 10 FPKM values. **c** KEGG glucosinolate biosynthesis pathway (*ath00966*) visualized using KEGG Mapper (Color Pathway). Reactions associated with differentially expressed genes identified in this study are highlighted in red. Annotated pathway genes not detected as differentially expressed are shown in green

biosynthesis of JA, which plays a key role in plant resistance against herbivores [20, 22]. Thus, our analysis provides a hint towards important reorganisation of the transcriptome in response to the exDNA treatment and to reinforce the response against herbivores.

The application of exDNA leads to a priming response in glucosinolate metabolism upon herbivory

Besides the pivotal role of GSLs in immunity, the expression profile described by the encoding transcripts (cluster 5) was consistent with the concept of defence priming, where an initial stimulus prepares the plant for a faster and stronger response to subsequent challenges [49, 50]. Then, to gain deeper insights into the contribution of GSL to the mechanism of exDNA-IR against thrips, the degree of reconfiguration in the GSLs pathway was investigated. Transcript changes were found for genes associated within both the aliphatic and indolic metabolic branches. Quantitatively, up to 20-fold enrichment of the glucosinolate pathways was observed in cluster 5, and this enrichment was associated with higher expression of 14 aliphatic and indolic GSL genes in exDNA-infested plants compared with infested control plants (Fig. 2a, b), showing that the application of exDNA induces a substantial reconfiguration of the entire pathway to increase the production of GSL upon thrips infestation.

To test whether the transcriptional changes on the GSLs pathway is followed by a higher accumulation of metabolites, key indolic and aliphatic glucosinolates, including glucobrassicin, glucohirsutin, glucoraphanin, and neoglucobrassicin, were quantified at 7 and 24 hpi by HPLC-MS/MS (Fig. 3a-b). Interestingly, all measured GSLs showed a significant accumulation in response to exDNA treatment at 7 hpi. However, indolic GSLs (glucobrassicin) and aliphatic GSLs (glucoraphanin) levels were significantly elevated in exDNA-treated plants compared to other groups of plants, showing a priming profile (Fig. 3a). The final concentration of GSLs at 24 hpi was similar between water and exDNA-treated plants, suggesting that the beneficial effect of the exDNA treatments stands on a faster production of GSLs (Fig. 3b).

Glucosinolates are central components sustaining the exDNA-IR

Our data suggests a critical role of both aliphatic and indolic GSLs in exDNA-induced immunity. Therefore, we hypothesised that exDNA-IR against thrips will fail in Arabidopsis mutants unable to accumulate GSLs. For this purpose, the *cyp83a1* and the *myb28/29* double mutant, compromised in aliphatic glucosinolate biosynthesis [39, 41], while the *cyp79b2/b3* double mutant, compromised in indolic biosynthesis [40], were selected as representative lines to address the contribution of each of the branches in the GSL biosynthesis pathway. Arabidopsis plants were water- or exDNA-treated 24 h before thrips infestation, and the measurement of the thrips feeding area at 4 dpi. As expected, exDNA treatment induced resistance in wild type plants (WT) [20]. However, exDNA-IR in *myb28/29* and *cyp83a1* mutants was abolished, showing a significant increase in the feeding leaf area in *cyp83a1* mutant treated plants (Fig. 4), while the *cyp79b2/b3* maintained exDNA-IR demonstrating that GSLs, especially aliphatic ones, mediate exDNA-IR in Arabidopsis against thrips.

Discussion

This study explores the molecular pathways contributing to the exDNA-IR against the herbivorous pest *F. occidentalis* through a comprehensive transcription analysis. Our findings show that exDNA treatment significantly alters the expression of numerous genes, specially from the lipid metabolism and in the presence of insect herbivory, exDNA treatment enriches the expression of genes associated with the glucosinolates pathway, known for their crucial role in plant defence against herbivorous threats [31, 51–54]. Moreover, we showed the higher accumulation of GSLs in exDNA-treated plants and confirmed the importance of indolic and aliphatic GSLs in exDNA-induced immunity using deficient mutants. Our study provides insight into defence pathways contributing to exDNA-IR against thrips herbivory.

Extracellular self-DNA treatment induces a significant alteration in the gene expression profiles of Arabidopsis plants (Fig. 1a). Previous research has described significant alterations in tomato gene expression following exDNA treatment with a broad modulation of genes associated with responses to biotic stress [32, 35]. Interestingly, a previous study on peach fruit reported that plants infected with the fungus *Rhizopus stolonifer*, as well as plants treated with exDNA and subsequently infected, exhibited a higher number of DEGs compared to plants treated solely with exDNA [14]. However, our study demonstrate that transcriptomic changes are primarily driven by the exDNA treatment itself rather than

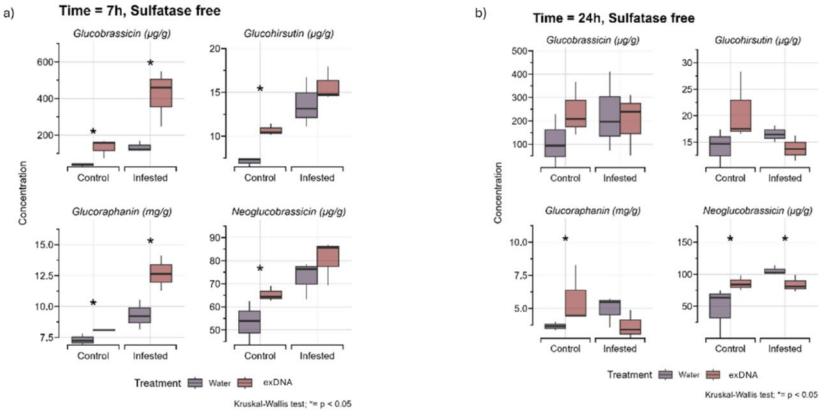

Fig. 3 Glucosinolate content in control and exDNA-treated plants under thrips infestation. **a** The glucosinolates quantitative levels in control and exDNA treated *Arabidopsis thaliana* plants with and without thrips infestation, 7 hpi and (**b**) 24 hpi, measured by targeted HPLC-MS/MS analysis (Kruskal-Wallis, Mann-Whitney; P-value < 0.05)

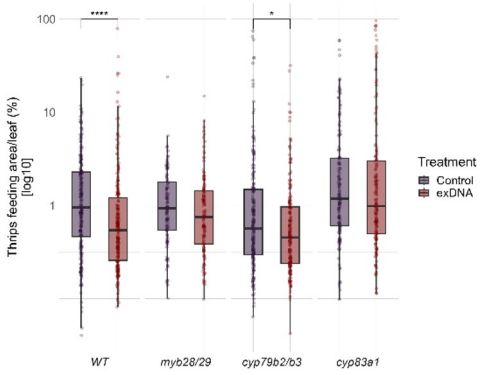

Fig. 4 Thrips feeding symptoms in exDNA-treated and control plants. The Percentage of thrips feeding area in WT Arabidopsis Col-0 and glucosinolate deficient mutants *myb28/29 cyp79b2/b3* and *cyp83a1* in exDNA-treated and control plants 4 dpi. Each plant ($n = 10$ per genotype) was infested with 15 adult thrips. Data from at least three independent experiments were pooled for statistical analysis (total observations ≈ 190). Statistical significance was assessed using Kruskal–Wallis followed by Mann–Whitney post hoc tests ($P < 0.05$)

infestation. Our functional annotation analysis revealed that most altered genes are associated with the plant stress response, and this observation supports the proposed role of exDNA as a danger signal, triggering plant responses, as previously suggested by several authors [7, 32, 33, 35].

While exDNA treatment increases the enrichment of fatty acids, thrips infestation in exDNA-treated plants enhances the enrichment of GSLs and α-linolenic acid metabolic pathways. These pathways are crucial for defending against chewing and pierce-sucking herbivores, as previously shown [22, 27, 31, 55]. Fatty acids, particularly α-linolenic acid, are the precursors for the octadecane pathway, a major contributor to JA synthesis in plant defence responses [56, 57]. Although our study shows no differences in JA gene expression after exDNA treatment alone, exDNA-treated plants infested with thrips exhibited a significant increase in the enrichment of JA biosynthesis genes (supplementary table S1). Previous studies have shown that JA plays a crucial role in the basal resistance against thrips [22, 58–60]. This also aligns with our previous findings on JA induction following exDNA treatment and infestation [20], indicating a critical role not only in the basal resistance, but also in the induced resistance.

Our results have displayed a contrasting enrichment of genes linked to serine metabolism in exDNA-infested plants (Supplementary Table S2). Serine plays a crucial role in various physiological processes, particularly in response to both biotic and abiotic stresses [61]. In plants, it is synthesized through three main pathways: the phosphorylated pathway, the glycerate pathway, and the glycolate pathway [62]. Here, our findings showed an enrichment in genes related to the phosphorylated pathway (PDGH), particularly, *PDGH3* in cluster 1 and *PDGH2* in cluster 5. It has been shown that the genes *PDGH1*, *PDGH2*, and *PDGH3* exhibit an antagonistic relationship, serving as positive and negative regulators within the pathway [63]. In this line, we have observed the lower enrichment in the negative regulator PDGH3, possibly linked to the heightened enriment of PDGH2. Serine is crucial for sulphate assimilation, thereby influencing glucosinolate metabolism. Additionally, it acts as a precursor for derivatives like methionine and tryptophan, which serve as major precursors for aliphatic and indolic glucosinolates [61, 64]. Therefore, it is tempting to speculate a possible regulation between serine metabolisms and glucosinolate accumulation in exDNA-treated plants infested with thrips. Additionally, we have also identified a notable suppression in genes associated with the glyoxylate pathway, specifically *AGT2*, *AGT*, *GGT1*, and *SHM6*. A recent study has proposed a negative interaction between serine accumulation through the glyoxylate pathway and sulphur (S) metabolism [61]. Therefore,

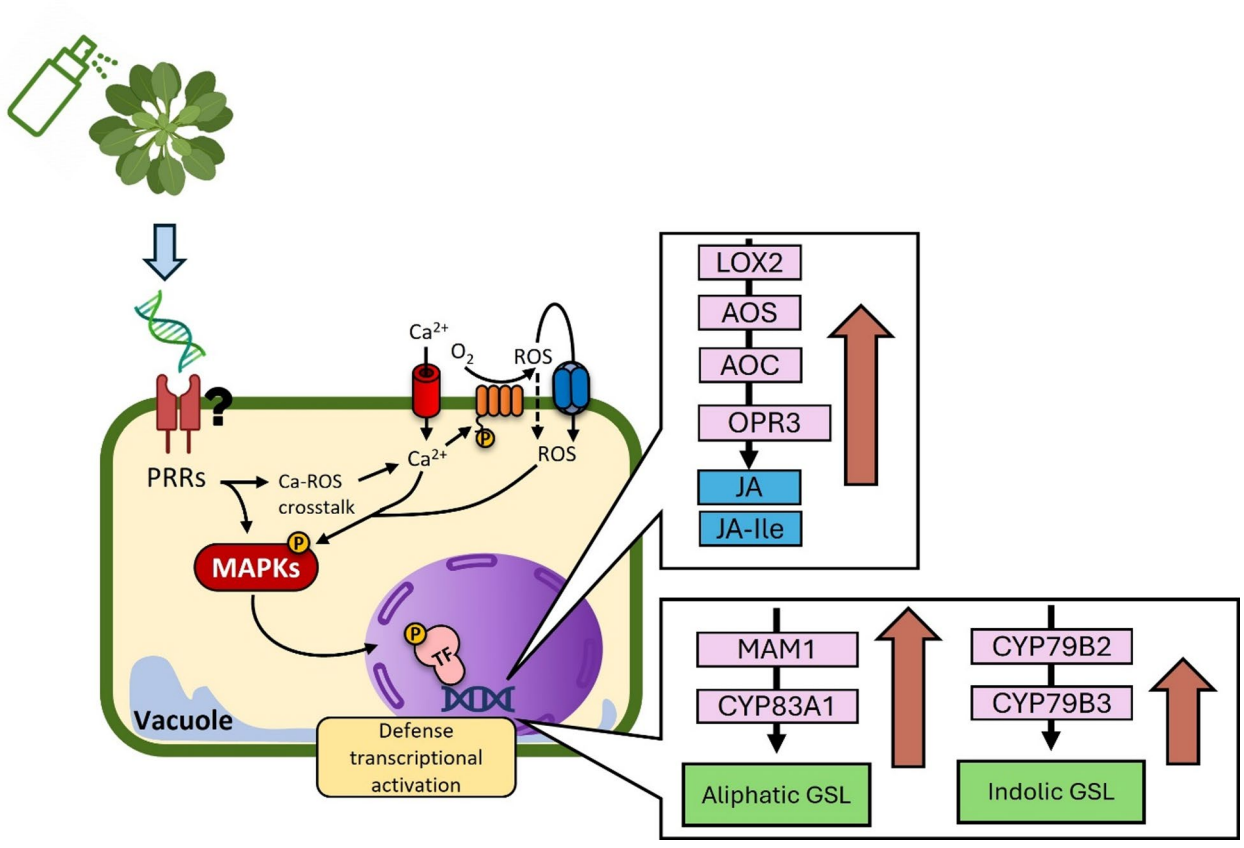

Fig. 5 Graphical overview of exDNA-triggered defence responses leading to glucosinolate accumulation during thrips infestation. Application of exDNA is proposed to trigger early defence-associated signalling events, ROS production, calcium influx, and MAP kinase activation, as previously reported for exDNA responses. These early signalling events are associated with activation of JA-related pathways, which in turn promote the transcriptional induction of GSL biosynthetic genes, with a predominant enrichment of the aliphatic branch. Upon thrips infestation, exDNA-treated plants display enhanced expression of GSL biosynthetic genes and increased accumulation of GSLs, contributing to induced resistance against thrips

we hypothesize that the reduced expression in the glyoxylate pathway implies an increased metabolic flux from serine to sulphur assimilation pathway, further linking it to the regulation of glucosinolate.

GSLs are key components of plant defence against herbivory. While GSLs are constitutively produced and stored in an inactive form, GSLs are rapidly hydroylzed upon tissue damage by the enzyme myrosinase, generating active compounds that are toxic to herbivores [29–31, 65].

Here, we showed that GSLs mediate exDNA-IR against thrips. Transcriptomic analysis revealed strong induction of genes involved in the two main GSLs biosynthetic pathways in plants treated with exDNA and those subsequently infested with thrips, with a predominant enrichment of the aliphatic branch. In particular, the expression of BCAT4, MAM1, IIL1, CYP79F1 and CYP83A was upregulated in exDNA-treated plants compared with their respective controls, supporting the contribution of aliphatic GSL biosynthesis during exDNA-IR (Fig. 5). Additionally, JA regulates the accumulation of secondary metabolites such as glucosinolates against spider mites [51, 66]. Thus, it is reasonable to speculate that JA could regulate the accumulation of GSL in exDNA-treated plants upon thrips infestation.

Consistent with this transcriptional evidence, genetic analyses further demonstrated that exDNA-IR against thrips is abolished in aliphatic GSL-deficient mutants at 4 dpi, highlighting the essential role of the glucosinolate pathway in mediating exDNA-induced immunity.

To determine which GSL branch mediates exDNA-IR, we employed mutants deficient in both major glucosinolate pathways, *cyp79b2/b3* and *cyp83a1*, which disrupt indolic and aliphatic GSL biosynthesis respectively, and *myb28/myb29*, lacking the key transcription factors that regulate aliphatic glucosinolate biosynthesis [39–41, 67]. Although GSL-deficient plants did not exhibit increased basal susceptibility compared to the controls, exDNA treatment failed to induce resistance in mutants lacking aliphatic GSLs (*myb28/29* and *cyp83a1*). In contrast, *cyp79b2/b3* partially retained exDNA-IR, suggesting that aliphatic rather than indolic GSLs are required for this defence response. These results are consistent with the transcriptomic data, in which genes associated with

the aliphatic GSL branch were more enriched following exDNA treatment. Together, these results indicate that aliphatic GSLs are needed for exDNA-IR, whereas indolic GSLs are not necessary for this response.

Both indolic and aliphatic glucosinolates contribute to plant resistance against pests and herbivores, but their relative importance varies among species. For example, indolic GSLs plays a crucial role against aphids (*Myzus persicae*) [53] and mite herbivory (*Tetranychus urticae*) [51, 66], while resistance to the lepidopteran *Mamestra brassicae* is mediated by aliphatic GSLs The Egyptian cotton leafworm (*Spodoptera littoralis*) is sensitive to both classes [54].

Natural variation studies have shown that resistance of Arabidopsis to western flower thrips is associated with specific aliphatic glucosinolate chemotypes rather than total glucosinolate levels, with genetic variation in the MAM and AOP loci influencing thrips feeding damage. In particular, hydroxylated aliphatic glucosinolates produced via AOP3 activity have been linked to reduced thrips herbivory [68]. These findings are consistent with our results showing transcriptional activation of aliphatic glucosinolate biosynthetic genes and the requirement of aliphatic glucosinolates for exDNA-induced resistance.

Conclusion

In this study, through transcriptomic, metabolic and genetic analysis we explore the defence mechanisms underlying exDNA-IR against *F. occidentalis*. We demonstrate that exDNA enhances plant defence responses upon thrips infestation, by promoting gene expression associated with stress and secondary metabolism.

RNA-Seq analysis revealed that exDNA treatment alone is sufficient to trigger transcriptional changes, supporting the role of exDNA as a DAMP. Upon thrips infestation, exDNA treated plants showed activation of GSL biosynthetic pathways, especially towards the aliphatic branch. This transcriptional reconfiguration was followed by accumulation of GSLs in infested exDNA treated plants.

Genetic analysis further demonstrated that exDNA induced resistance depends mainly on aliphatic glucosinolates. The loss of exDNA-IR in aliphatic GSL deficient mutants, but not in indolic GSL deficient plants, suggests aliphatic GSLs as mediators of this induced defence.

Overall, our work provides new evidence into how plants integrate extracellular self-DNA signals to activate inducible chemical defences and highlights exDNA as a key regulator of herbivore resistance. Our findings advance the understanding of exDNA as a potential DAMP signal that enhances plant resistance and shed light on the underlying mechanisms involved.

Abbreviations

DAMPs	Damage–associated molecular patterns
DAVID	Database for Annotation, Visualization, and Integrated Discovery
DEGs	Differentially Expressed Genes
dpi	Days post–infestation
ETI	Effector–triggered immunity
exDNA	Extracellular DNA
exDNA-IR	ExDNA–induced resistance
FPKMs	Fragments Per Kilobase Million
GSL	Glucosinolate
GO	Gene Ontology
GOX	Glycolate Oxidase
hpi	Hours post–infestation
JA	Jasmonic acid
KCS	β–Ketoacyl–CoA synthetase
KEGG	Kyoto Encyclopedia of Genes and Genomes
LACS	Long–chain acyl–CoA synthetase
LSD	Least significant difference
MDS	Multidimensional scaling
MRM	Multiple Reaction Monitoring
NASC	Nottingham Arabidopsis Stock Centre
PAMPs	Pathogen–associated molecular patterns
PDGH	Phosphorylated pathway
PRRs	Pattern recognition receptors
PTI	Pattern–triggered immunity
RBCS	Ribulose bisphosphate carboxylase (small chain) family protein
RIN	RNA integrity number
ROS	Reactive oxygen species
TSWV	Tomato spotted wilt virus
UPLC	Ultra–performance liquid chromatography
VOCs	Volatile Organic Compounds
VLCFAs	Very long–chain fatty acids
WT	Wild type

Supplementary Information

The online version contains supplementary material available at https://doi.org/10.1186/s12870-026-08533-7.

Supplementary Material 1. Figure S1. Enriched GO terms based on heatmap clusters sorted by fold enrichment levels and number of genes. a) The top enriched GO terms for Cluster 1. b) The top enriched GO terms for Cluster 3. Point size indicates the number of genes associated with each GO term, and color represents fold enrichment values ranging from low (blue) to high (red). Fold Enrichment is defined as the percentage of genes in our list belonging to a pathway divided by the corresponding percentage in the background. GO and pathway enrichment analysis were carried out using ShinyGO software v 0.77. Supplementary Table S1. List of enriched genes observed in cluster1, pathway: Glyoxylate and dicarboxylate metabolism, cluster 3, pathway: Fatty acid elongation, Fatty acid metabolism, Fatty acid biosynthesis and cluster 5, pathway: Glucosinolate biosynthesis and alpha-Linolenic acid metabolism. KEGG pathway analysis was performed using the DAVID Bioinformatics Resources. Supplementary Table S2. List of enriched genes in Pathway: Glycine, serine and threonine metabolism, in cluster 5 and 1. KEGG pathway analysis was performed using the DAVID Bioinformatics Resources.

Acknowledgements

We gratefully acknowledge the technical assistance provided by the Scientific Instrumentation Service (SCIC) of the Universitat Jaume I. We are thankful to Prof. Jonathan Gershenzon for sending the Arabidopsis mutant seeds essential for this work.

Authors' contributions

VF, JG, and LR designed the experiments. LR, JG and IV performed the experiments. AG, LR, IV, and JG analysed the data and interpreted the results. All authors contributed to the writing and revision of the manuscript.

Funding
This work was financially supported by the Spanish Government through the PID2023-149147OB-I00 grant funded by MCIN/ AEI/10.13039/501100011033, and the CDEIGENT/2018/015 fellowship from the Generalitat Valenciana.

Data availability
The data supporting the findings of this study are available in the Supplementary Material associated with this article. RNAseq data has been submitted into NCBI Sequence Read Archive (SRA) with accession number: PRJNA1373521.

Declarations

Ethics approval and consent to participate
Not applicable.

Consent for publication
Not applicable.

Competing interests
The authors declare no competing interests.

Received: 25 November 2025 / Accepted: 5 March 2026
Published online: 12 March 2026

References

1. Gust AA, Pruitt R, Nürnberger T. Sensing Danger: Key to Activating Plant Immunity. Trends Plant Sci. 2017;22:779–91. https://doi.org/10.1016/j.tplants.2017.07.005.
2. Cui H, Tsuda K, Parker JE. Effector-triggered immunity: from pathogen perception to robust defense. Annu Rev Plant Biol. 2015;66:487–511. https://doi.org/10.1146/annurev-arplant-050213-040012.
3. Hou S, Liu Z, Shen H, Wu D. Damage-Associated Molecular Pattern-Triggered Immunity in Plants. Front Plant Sci. 2019;10. https://doi.org/10.3389/fpls.2019.00646.
4. Naveed ZA, Wei X, Chen J, Mubeen H, Ali GS. The PTI to ETI Continuum in Phytophthora-Plant Interactions. Front Plant Sci. 2020;11. https://doi.org/10.3389/fpls.2020.593905.
5. Tanaka K, Heil M. Damage-Associated Molecular Patterns (DAMPs) in plant innate immunity: Applying the danger model and evolutionary perspectives. Annu Rev Phytopathol. 2021. https://doi.org/10.2307/5240.
6. Quintana-Rodriguez E, Duran-Flores D, Heil M, Camacho-Coronel X. Damage-associated molecular patterns (DAMPs) as future plant vaccines that protect crops from pests. Sci Hortic. 2018;237:207–20. https://doi.org/10.1016/j.scienta.2018.03.026.
7. Barbero F, Guglielmotto M, Capuzzo A, Maffei ME. Extracellular self-DNA (esDNA), but not heterologous plant or insect DNA (etDNA), induces plasma membrane depolarization and calcium signaling in lima bean (Phaseolus lunatus) and maize (Zea mays). Int J Mol Sci. 2016;17. https://doi.org/10.3390/ijms17101659.
8. Duran-Flores D, Heil M. Growth inhibition by self-DNA: a phenomenon and its multiple explanations. New Phytol. 2015;207:482–5.
9. Mazzoleni S, Cartenì F, Bonanomi G, Senatore M, Termolino P, Giannino F, et al. Inhibitory effects of extracellular self-DNA: a general biological process? New Phytol. 2015;206:127–32. https://doi.org/10.1111/nph.13306.
10. Mazzoleni S, Bonanomi G, Incerti G, Chiusano ML, Termolino P, Mingo A, et al. Inhibitory and toxic effects of extracellular self-DNA in litter: a mechanism for negative plant – soil feedbacks ? New Phytol. 2015;205:1195–210.
11. Gamir J, Vega-Muñoz I, Rassizadeh L, Heil M. On the quest for undiscovered plant DNA receptors. Trends Plant Sci. 2025;30:1226–36. https://doi.org/10.1016/j.tplants.2025.04.011.
12. Durán-Flores D, Heil M. The CpG-dependent plant immune response to self-DNA triggers defence hormone signalling and improves fitness. Res Sq. 2023. https://doi.org/10.21203/rs.3.rs-2649049/v1.
13. Ferrusquía-Jiménez N, Chandrakasan G, Torres-Pacheco I, Rico-García E, Feregrino-Pérez AA, Guevara-González RG. Extracellular DNA: A Relevant Plant Damage - Associated Molecular Pattern (DAMP) for Crop Protection Against Pests — A Review. J Plant Growth Regul. 2021. https://doi.org/10.1007/s00344-020-10129-w.
14. Li C, Wang K, Zou Y, Lei C, Chen Z. Extracellular self-DNA induced a PTI-related local defence against Rhizopus rot in postharvest peach fruit. Postharvest Biol Technol. 2023;200:112306. https://doi.org/10.1016/j.postharvbio.2023.112306.
15. Rassizadeh L, Cervero R, Flors V, Gamir J. Extracellular DNA as an elicitor of broad-spectrum resistance in Arabidopsis thaliana. Plant Sci. 2021;312:111036. https://doi.org/10.1016/j.plantsci.2021.111036.
16. Zhou X, Gao H, Zhang X, Khashi u Rahman M, Mazzoleni S, Du M, et al. Plant extracellular self-DNA inhibits growth and induces immunity via the jasmonate signaling pathway. Plant Physiol. 2023;192:2475–91. https://doi.org/10.1093/plphys/kiad195.
17. Zou Y, Yang S, Ren Q, Chen J, Wang K, Li C, et al. Extracellular self-DNA as a DAMP signal for induced systemic resistance to anthracnose rot in postharvest loquat fruit via EjRAV2-EjERF39 module. Postharvest Biol Technol. 2024;216:113023. https://doi.org/10.1016/j.postharvbio.2024.113023.
18. Zou Y, Li C, Xiang F, Xia Y, Zhou M, Wang K et al. Exploring sDNA recognition and PTI activation in postharvest peach fruit through DNA methylation into host defense. 2025. https://doi.org/10.1016/j.postharvbio.2025.113404.
19. Vega-Muñoz I, Herrera-Estrella A, Martínez-de la Vega O, Heil M. ATM and ATR, two central players of the DNA damage response, are involved in the induction of systemic acquired resistance by extracellular DNA, but not the plant wound response. Front Immunol. 2023;May:1–25. https://doi.org/10.3389/fimmu.2023.1175786.
20. Rassizadeh L, Cañadas E, Cervero R, Flors V, Gamir J. Extracellular DNA induces resistance against Frankliniella occidentalis through callose accumulation. J Pest Sci. 2004;2024. https://doi.org/10.1007/s10340-023-01733-2.
21. Reitz SR, Gao Y, Kirk WDJ, Hoddle MS, Leiss KA, Funderburk JE. Invasion Biology, Ecology, and Management of Western Flower Thrips. Annu Rev Entomol. 2019;65:17–37. https://doi.org/10.1146/annurev-ento-011019-024947.
22. Abe H, Shimoda T, Ohnishi J, Kugimiya S, Narusaka M, Seo S, et al. Jasmonate-dependent plant defense restricts thrips performance and preference. BMC Plant Biol. 2009;9. https://doi.org/10.1186/1471-2229-9-97.
23. Berens ML, Berry HM, Mine A, Argueso CT, Tsuda K. Evolution of Hormone Signaling Networks in Plant Defense. Annu Rev Phytopathol. 2017;55:401–25. https://doi.org/10.1146/annurev-phyto-080516-035544.
24. Mokh S, Portoles T, Gamir J. Analytical approaches for volatile organic compounds to understand plant communication. Curr Plant Biol. 2025;44:100547. https://doi.org/10.1016/J.CPB.2025.100547.
25. Verhage A, van Wees SCM, Pieterse CMJ. Plant Immunity: It's the Hormones Talking, But What Do They Say? Plant Physiol. 2010;154:536–40. https://doi.org/10.1104/PP.110.161570.
26. War AR, Paulraj MG, Ahmad T, Buhroo AA, Hussain B, Ignacimuthu S, et al. Mechanisms of plant defense against insect herbivores. Plant Signal Behav. 2012;7. https://doi.org/10.4161/PSB.21663.
27. Howe GA, Jander G. Plant Immunity to Insect Herbivores. Annu Rev Plant Biol. 2008;59:41–66. https://doi.org/10.1146/annurev.arplant.59.032607.092825.
28. Divekar PA, Narayana S, Divekar BA, Kumar R, Gadratagi BG, Ray A, et al. Plant Secondary Metabolites as Defense Tools against Herbivores for Sustainable Crop Protection. Int J Mol Sci. 2022;23. https://doi.org/10.3390/IJMS23052690.
29. Halkier BA, Gershenzon J. Biology and Biochemistry of Glucosinolates. Annu Rev Plant Biol. 2006;57:303–33. https://doi.org/10.1146/annurev.arplant.57.032905.105228.
30. Mitreiter S, Gigolashvili T. Regulation of glucosinolate biosynthesis. J Exp Bot. 2021;72:70–91. https://doi.org/10.1093/JXB/ERAA479.
31. Textor S, Gershenzon J. Herbivore induction of the glucosinolate-myrosinase defense system: Major trends, biochemical bases and ecological significance. Phytochem Rev. 2009;8:149–70. https://doi.org/10.1007/S11101-008-9117-1.
32. Barbero F, Guglielmotto M, Islam M, Maffei ME. Extracellular Fragmented Self-DNA Is Involved in Plant Responses to Biotic Stress. Front Plant Sci. 2021;12:1–17. https://doi.org/10.3389/fpls.2021.686121.
33. Duran-Flores D, Heil M. Extracellular self-DNA as a damage-associated molecular pattern (DAMP) that triggers self-specific immunity induction in plants. Brain Behav Immun. 2018;72:78–88. https://doi.org/10.1016/j.bbi.2017.10.010.
34. Vega-Muñoz I, Feregrino-Pérez AA, Torres-Pacheco I, Guevara-González RG, Feregrino-Perez AA, Torres-Pacheco I, et al. Exogenous fragmented DNA acts as a damage-associated molecular pattern (DAMP) inducing changes in CpG DNA methylation and defence-related responses in Lactuca sativa. Funct Plant Biol. 2018. https://doi.org/10.1071/FP18011.

35. Chiusano ML, Incerti G, Colantuono C, Termolino P, Palomba E, Monticolo F, et al. Arabidopsis thaliana Response to Extracellular DNA: Self Versus Nonself Exposure. Plants. 2021;10. https://doi.org/10.3390/plants10081744.
36. Yakushiji S, Ishiga Y, Inagaki Y, Toyoda K, Shiraishi T, Ichinose Y. Bacterial DNA activates immunity in Arabidopsis thaliana. J Gen Plant Pathol. 2009;75:227–34. https://doi.org/10.1007/s10327-009-0162-4.
37. Carbajal-Valenzuela IA, Guzmán-Cruz R, González-Chavira MM, Medina-Ramos G, Serrano-Jamaica LM, Torres-Pacheco I, et al. Response of Plant Immunity Markers to Early and Late Application of Extracellular DNA from Different Sources in Tomato (Solanum lycopersicum). Agriculture. 2022;12. https://doi.org/10.3390/agriculture12101587.
38. Beekweelder J, van Leeuwen W, van Dam NM, Bertossi M, Grandi V, Mizzi L, et al. The impact of the absence of aliphatic glucosinolates on insect herbivory in Arabidopsis. PLoS ONE. 2008;3. https://doi.org/10.1371/journal.pone.0002068.
39. Sønderby IE, Hansen BG, Bjarnholt N, Ticconi C, Halkier BA, Kliebenstein DJ. A systems biology approach identifies a R2R3 MYB gene subfamily with distinct and overlapping functions in regulation of aliphatic glucosinolates. PLoS ONE. 2007;2. https://doi.org/10.1371/journal.pone.0001322.
40. Zhao Y, Hull AK, Gupta NR, Goss KA, Alonso J, Ecker JR, et al. Trp-dependent auxin biosynthesis in Arabidopsis: Involvement of cytochrome P450s CYP79B2 and CYP79B3. Genes Dev. 2002;16:3100–12. https://doi.org/10.1101/gad.1035402.
41. Hemm MR, Ruegger MO, Chapple C. The arabidopsis ref2 mutant is defective in the gene encoding CYP83A1 and shows both phenylpropanoid and glucosinolate phenotypes. Plant Cell. 2003;15:179–94. https://doi.org/10.1105/tpc.006544.
42. Schindelin J, Arganda-Carreras I, Frise E, Kaynig V, Longair M, Pietzsch T, et al. Fiji: an open-source platform for biological-image analysis. Nat Methods 2012. 2012;9:7. https://doi.org/10.1038/nmeth.2019.
43. Ojeda-Martinez D, Martinez M, Diaz I, Santamaria ME. Saving time maintaining reliability: A new method for quantification of Tetranychus urticae damage in Arabidopsis whole rosettes. BMC Plant Biol. 2020;20. https://doi.org/10.1186/s12870-020-02584-0.
44. Berg S, Kutra D, Kroeger T, Straehle CN, Kausler BX, Haubold C, et al. ilastik: interactive machine learning for (bio)image analysis. Nat Methods. 2019;16:1226–32. https://doi.org/10.1038/s41592-019-0582-9.
45. Garcia-Molina A, Marino G, Lehmann M, Leister D. Systems biology of responses to simultaneous copper and iron deficiency in Arabidopsis. Plant J. 2020;103:2119–38. https://doi.org/10.1111/TPJ.14887.
46. Crocoll C, Halkier BA, Burow M. Analysis and Quantification of Glucosinolates. Curr Protoc Plant Biol. 2016;1:385–409. https://doi.org/10.1002/cppb.20027.
47. Zhang G, Shan S, Wu Y, Huang S, Li D, Deng J, et al. The KCS gene is involved in the formation of chloroplast stromules and other physiological processes in jute (Corchorus capsularis L). Ind Crops Prod. 2019;141. https://doi.org/10.1016/J.INDCROP.2019.111781.
48. Zhao H, Kosma DK, Lü S. Functional Role of Long-Chain Acyl-CoA Synthetases in Plant Development and Stress Responses. Front Plant Sci. 2021;12:640996. https://doi.org/10.3389/FPLS.2021.640996.
49. Conrath U, Beckers GJM, Flors V, García-Agustín P, Jakab G, Mauch F, et al. Priming: Getting Ready for Battle Prime-A-Plant Group. Mol Plant Microbe Interact. 2006;19:1062–71. https://doi.org/10.1094/MPMI.
50. Martinez-Medina A, Flors V, Heil M, Mauch-Mani B, Pieterse CMJ, Pozo MJ, et al. Recognizing Plant Defense Priming. Trends Plant Sci. 2016;21:818–22. https://doi.org/10.1016/J.TPLANTS.2016.07.009.
51. Zhurov V, Navarro M, Bruinsma KA, Arbona V, Estrella Santamaria M, Cazaux M, et al. Reciprocal Responses in the Interaction between Arabidopsis and the Cell-Content-Feeding Chelicerate Herbivore Spider Mite. Plant Physiol. 2014;164:384–99. https://doi.org/10.1104/PP.113.231555.
52. Müller R, de Vos M, Sun JY, Sønderby IE, Halkier BA, Wittstock U, et al. Differential effects of indole and aliphatic glucosinolates on lepidopteran herbivores. J Chem Ecol. 2010;36:905–13. https://doi.org/10.1007/S10886-010-9825-Z.
53. Kim JH, Jander G. Myzus persicae (green peach aphid) feeding on Arabidopsis induces the formation of a deterrent indole glucosinolate. Plant J. 2007;49:1008–19. https://doi.org/10.1111/J.1365-313X.2006.03019.X.
54. Jeschke V, Kearney EE, Schramm K, Kunert G, Shekhov A, Gershenzon J, et al. How glucosinolates affect generalist lepidopteran larvae: Growth, development and glucosinolate metabolism. Front Plant Sci. 2017;8:310911. https://doi.org/10.3389/FPLS.2017.01995.
55. Wari D, Aboshi T, Shinya T, Galis I. Integrated view of plant metabolic defense with particular focus on chewing herbivores. J Integr Plant Biol. 2022;64:449–75. https://doi.org/10.1111/JIPB.13204.
56. Wasternack C, Song S. Jasmonates: biosynthesis, metabolism, and signaling by proteins activating and repressing transcription. J Exp Bot. 2017;68:1303–21. https://doi.org/10.1093/JXB/ERW443.
57. Bürger M, Chory J. Stressed Out About Hormones: How Plants Orchestrate Immunity. Cell Host Microbe. 2019;26:163–72. https://doi.org/10.1016/j.chom.2019.07.006.
58. Abe H, Ohnishi J, Narusaka M, Seo S, Narusaka Y, Tsuda S, et al. Function of jasmonate in response and tolerance of Arabidopsis to thrip feeding. Plant Cell Physiol. 2008;49:68–80. https://doi.org/10.1093/pcp/pcm168.
59. De Vos M, Van Oosten VR, Van Poecke RMP, Van Pelt JA, Pozo MJ, Mueller MJ, et al. Signal Signature and Transcriptome Changes of Arabidopsis During Pathogen and Insect Attack. Mol Plant Microbe Interact. 2007;18:923–37. https://doi.org/10.1094/MPMI-18-0923.
60. Mouden S, Leiss KA. Host plant resistance to thrips (Thysanoptera: Thripidae) – current state of art and future research avenues. Curr Opin Insect Sci. 2021;45:28–34. https://doi.org/10.1016/J.COIS.2020.11.011.
61. Rosa-Téllez S, Casatejada-Anchel R, Alcántara-Enguídanos A, Torres-Moncho A, Dohgri M, Martínez-Serra C, et al. Serine Metabolic Networks in Plants. Cham: Springer; 2023. https://doi.org/10.1007/124_2023_73.
62. Ros R, Muñoz-Bertomeu J, Krueger S. Serine in plants: biosynthesis, metabolism, and functions. Trends Plant Sci. 2014;19:564–9. https://doi.org/10.1016/J.TPLANTS.2014.06.003.
63. Casatejada-Anchel R, Muñoz-Bertomeu J, Rosa-Téllez S, Anoman AD, Nebauer SG, Torres-Moncho A, et al. Phosphoglycerate dehydrogenase genes differentially affect Arabidopsis metabolism and development. Plant Sci. 2021;306:110863. https://doi.org/10.1016/J.PLANTSCI.2021.110863.
64. Zimmermann SE, Blau S, Frerigmann H, Krueger S. The phosphorylated pathway of serine biosynthesis is crucial for indolic glucosinolate biosynthesis and plant growth promotion conferred by the root endophyte Colletotrichum tofieldiae. Plant Mol Biol. 2021;107:85–100. https://doi.org/10.1007/S11103-021-01181-5.
65. Hopkins RJ, Van Dam NM, Van Loon JJA. Role of Glucosinolates in Insect-Plant Relationships and Multitrophic Interactions. Annu Rev Entomol. 2009;54:57–83. https://doi.org/10.1146/annurev.ento.54.110807.090623.
66. Widemann E, Bruinsma K, Walshe-Roussel B, Rioja C, Arbona V, Saha RK, et al. Multiple indole glucosinolates and myrosinases defend Arabidopsis against Tetranychus urticae herbivory. Plant Physiol. 2021;187:116–32. https://doi.org/10.1093/plphys/kiab247.
67. Hirai MY, Sugiyama K, Sawada Y, Tohge T, Obayashi T, Suzuki A, et al. Omics-based identification of Arabidopsis Myb transcription factors regulating aliphatic glucosinolate biosynthesis. Proc Natl Acad Sci U S A. 2007;104:6478–83. https://doi.org/10.1073/PNAS.0611629104.
68. Arouisse B, Thoen MPM, Kruijer W, Kunst JF, Jongsma MA, Keurentjes JJB, et al. Bivariate GWA mapping reveals associations between aliphatic glucosinolates and plant responses to thrips and heat stress. Plant J. 2024;120:674–86. https://doi.org/10.1111/tpj.17009.

Publisher's note